Electronic Supplementary Material (ESI) for Journal of Materials Chemistry A.

Supplementary Information For

Realization of Anion Insertion Mechanism for High-Rate Electrochemical Energy Storage in High Crystallinity Few-layer Potassium Manganese Dioxide Nanosheets

Yifan Zhang[ab], Shicong Zhang[bc], Zhang Chen[a], Tao Li[c], Yaoyao Zhao[b], Fuqiang Huang[*b], and Tianquan Lin[*c]

[a] School of Materials Science and Engineering, Shanghai University, Shanghai 200444, China

[b] State Key Laboratory of High Performance Ceramics and Superfine Microstructure, Shanghai Institute of Ceramics, Chinese Academy of Sciences, Shanghai, 200050, PR China

[c] School of Materials Science and Engineering, Shanghai Jiao Tong University, 800 Dongchuan Road, Shanghai, 200240

Electrochemical Data

For a nonlinear Faradaic capacitor, the capacitance is obtained from the integrated form

$$C = \frac{\int dQ}{\int dV} \tag{1}$$

In the above, *Q* is the charge during the CV/GCD charging or discharging cycle, and V is the potential. In GCD test, since I is set constant, so the equation reduces to

$$C = \frac{\int dQ}{\int dV} = \frac{I\Delta t}{\Delta V} \tag{2}$$

In the above, the Δt is the charging or discharging time, and ΔV is the potential window. The specific capacitance is the capacitance divided by the mass of the electrode

$$C = \frac{I}{m(\Delta V/\Delta t)} \tag{3}$$

The volumetric capacitance is likewise obtained by dividing capacitance by the volume of the electrode.

The rate independent current and diffusion-limited current are evaluated through Eq (4)[1], we write

$$i = k_1 v + k_2 v^{1/2} \tag{4}$$

Where the two terms arise from the rate-independent component and the diffusion-limited component of capacitance, respectively. Surface capacitive contribution can be calculated by this equation.

EQCM Data

The change of Sauerbrey mass converts into the frequency change of the quartz crystal by Sauerbrey's equation[2] through Dfind software (Biolin Scientific AB, Sweden).

$$m_f = -\frac{c}{n}\Delta f_n \tag{5}$$

In the above, *c* is a constant related to crystal sensitivity factors, *n* is the frequency

multiplier, and $^{\Delta f_n}$ is the change of n frequency multiplication. For the quartz sensor with the reference harmonic frequency of 5 MHz we used, C is 17.7 ng Hz^{-1} cm^{-2}. In this study, the Sauerbrey mass was all calculated through three frequency multiplication, and the area is 0.785 cm^2 (a circle with a diameter of 10 mm). The equation can be written as Eq (6)

$$m_f = -4.6315\Delta f_3 \text{ (ng)} \quad (6)$$

The exchanged molecular weight of ion (M_w, g/mol e^-) converts the change of Sauerbrey mass and the change of charge at the same time. The equation can be written as Eq (7)

$$M_w = F\frac{dm_f}{dQ} \quad (7)$$

In the above, *F* is Faraday constant, which is 96485 C mol^{-1}. The $^{dm_f/dQ}$ can be calculated by Sauerbrey mass *vs.* charge plot.

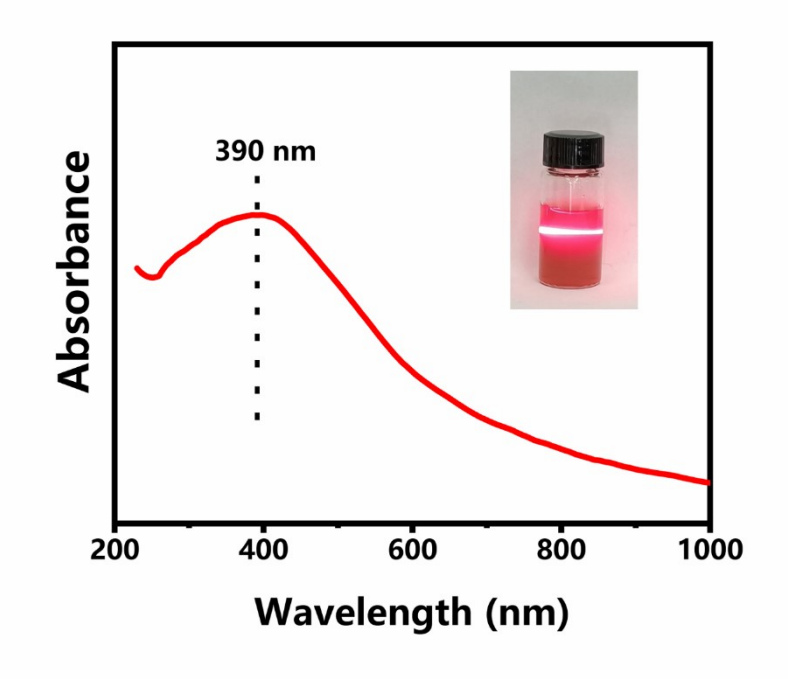

Fig. S1 UV-vis spectra of NS-KMnO and photograph of the Tynall phenomenon (insert).

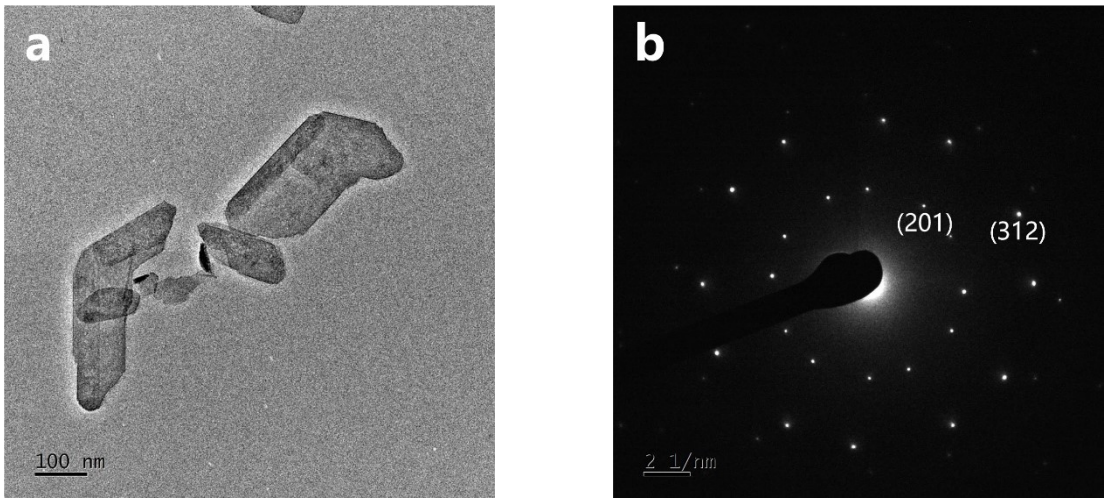

Fig. S2 TEM image (a) of NS-KMnO and corresponding SAED patterns(b). There are two sets of identical diffraction spots, indicating double-layer nanosheet.

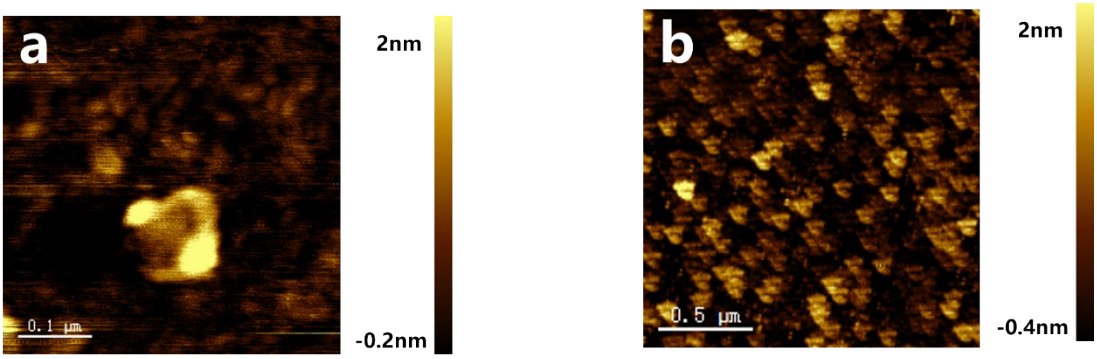

Fig. S3 AFM images of NS-KMnO. The range of thickness is from 0.5 to 3 nm, which the range of layer is from 1 to 5.

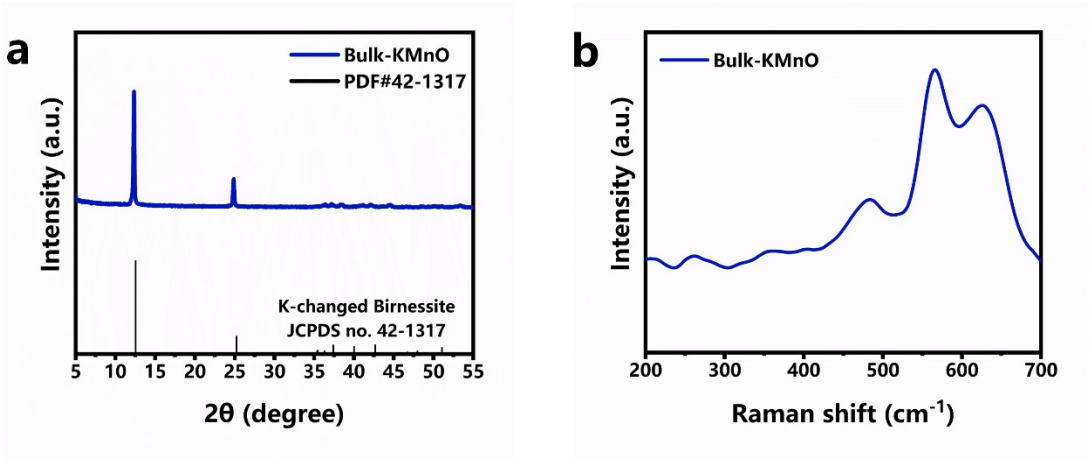

Fig. S4 Structure Characterization of Bulk-KMnO. (a) XRD patterns of Bulk-KMnO (blue line) and JCPDS no. 42-1317 (black line). (b) Raman scattering spectra of Bulk-KMnO. There are no other peaks except the Mn-O stretching vibration.

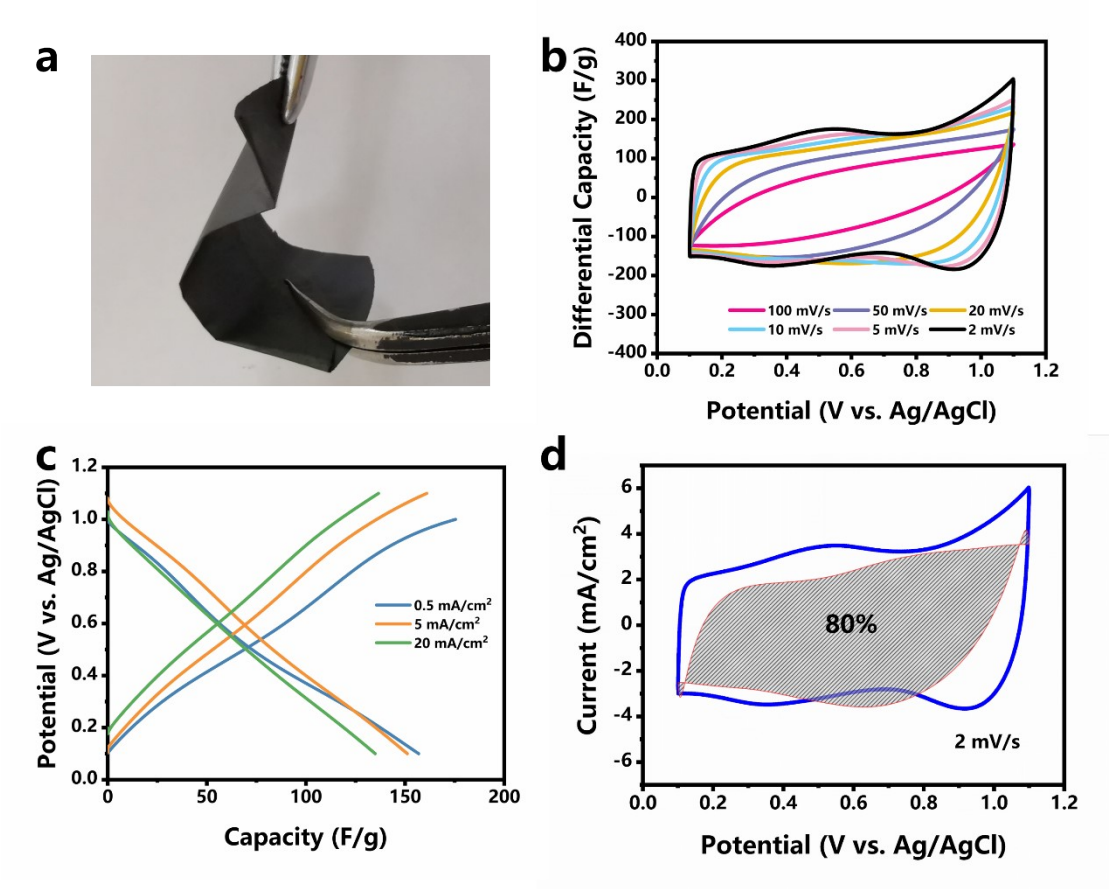

Fig. S5 Electrochemical Characterization of NS-KMnO. (a) Photographs showing flexible NS-KMnO@SWCNTs electrode. (b) CV curves of NS-KMnO with mass loading of 9.9 mg/cm^2 at scan rates of 2-100 mV/s. Here, current is normalized by scan rate *v*. (c) CC curves of NS-KMnO with mass loading of 9.9 mg/cm^2 at different current densities of 0.5-20 mA/cm2. (d) CV curve of NS-KMnO with mass loading of 9.9 mg/cm^2 with shadowed area respresenting the surface capacitive contribution.

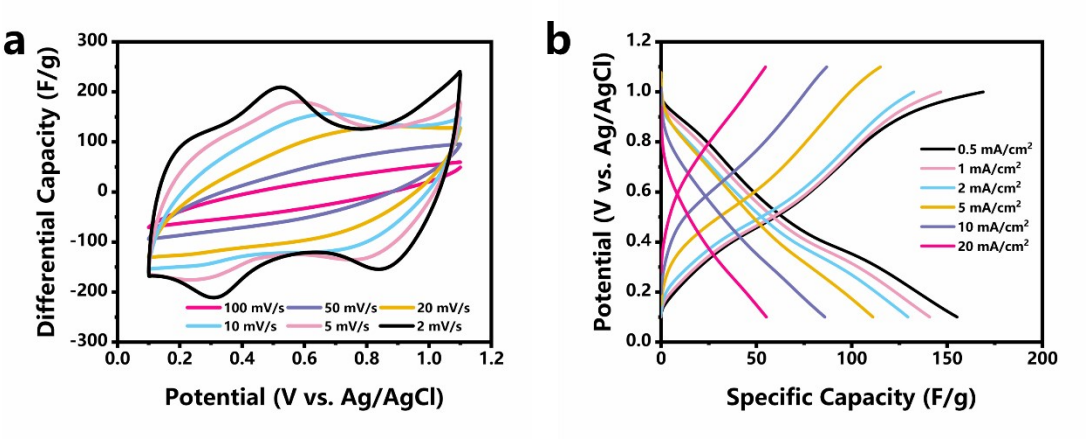

Fig. S6 Electrochemical Characterization of Bulk-KMnO with mass load of 9.7 mg cm^{-2}.

(a) CV curves at scan rates of 2-100 mV s^{-1}. Here, current is normalized by scan rate *v*.

(b) CC curves at different current densities of 0.5-20 mA cm^{-2}.

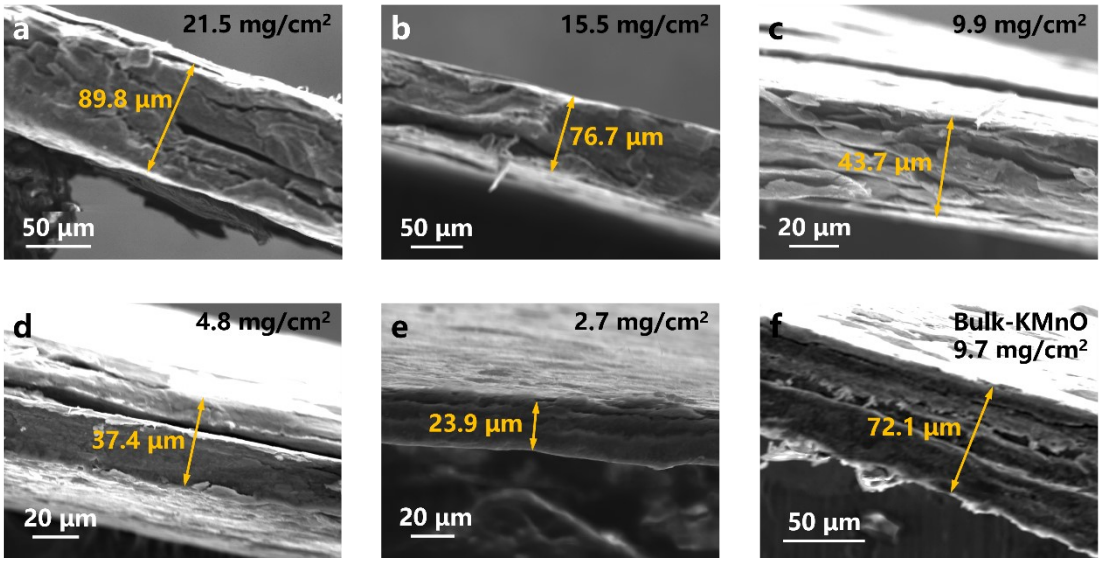

Fig. S7 SEM images of electrode with different mass loading. (a-e) NS-KMnO with mass loading from 21.5 to 2.7 mg cm^{-2}, and the thickness is marked by yellow words. (f) Bulk-KMnO with mass loading of 9.7 mg cm^{-2}, and the thickness is marked by yellow words.

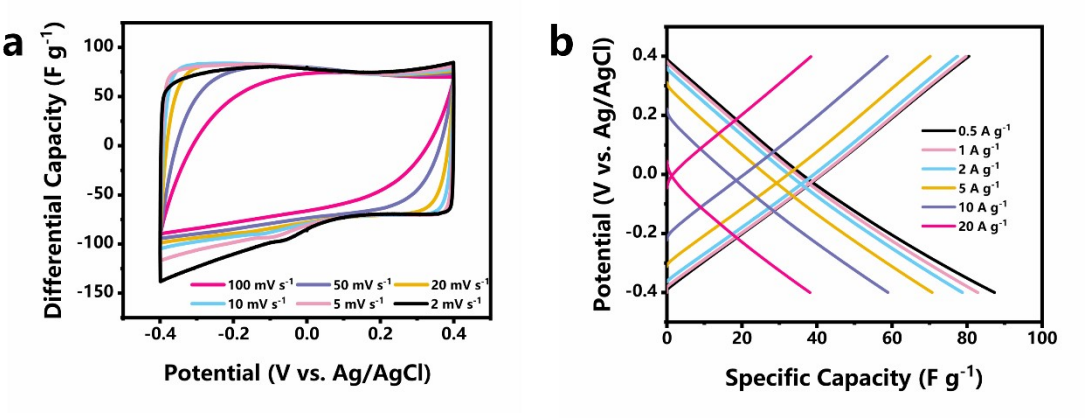

Fig. S8 Electrochemical characterization of YP-50 in three-electrode electrochemical cells. (a) CV curves at scan rates of 2-100 mV s^{-1}. Here, current is normalized by scan rate v. (b) CC curves at different current densities of 0.5-20 A g^{-1}.

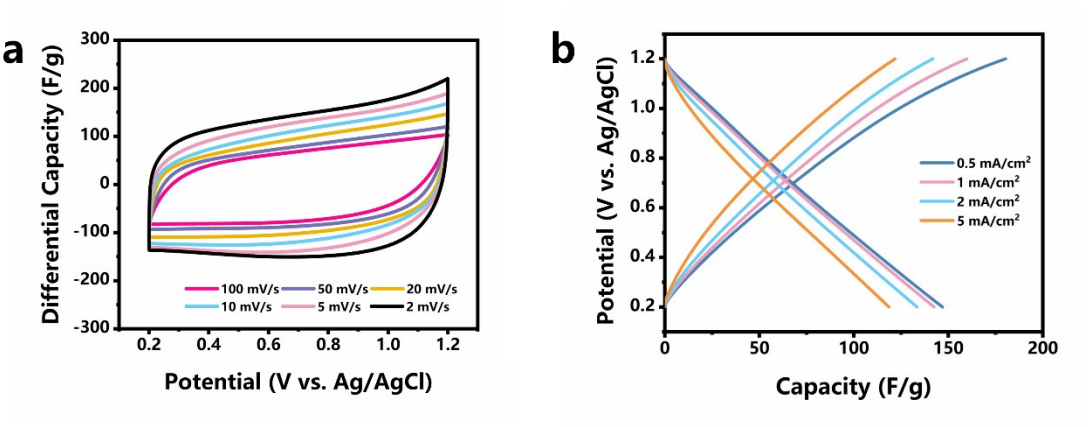

Fig. S9 Electrochemical Characterization of YP-50 electrode in three . (a) CV curves at scan rates of 2-100 mV s^{-1}. Here, current is normalized by scan rate *v*. (b) CC curves at different current densities of 0.5-20 mA cm^{-2}.

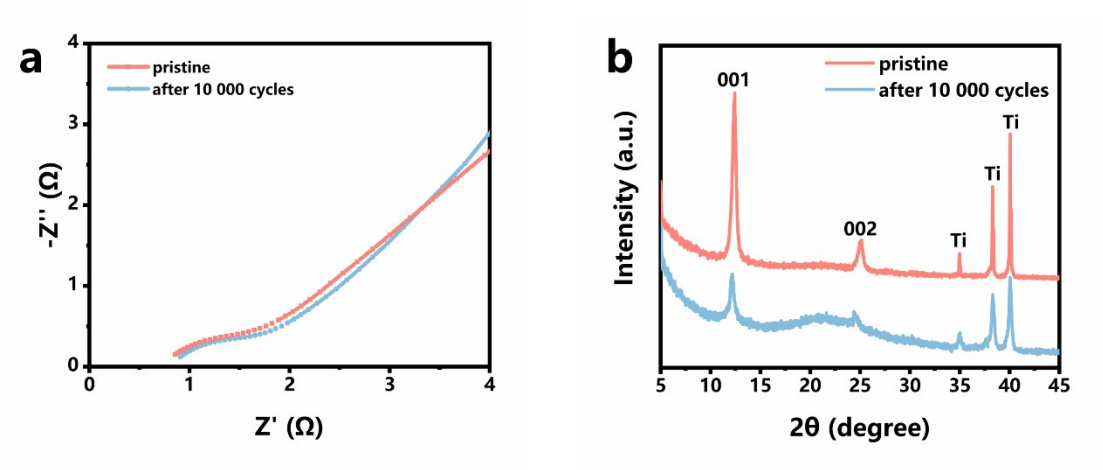

Fig. S10 Failure mechanism analysis. (a) Nyquist plot of NS-KMnO//YP-50 asymmetric supercapacitor at pristine (pink line) and after 10,000 cycles (blue line). It shows a little change in the structure of electrode. (b) XRD patterns of NS-KMnO electrode at pristine (pink line) and after 10,000 cycles (blue line). The crystallinity was reduced after 10,000 cycles.

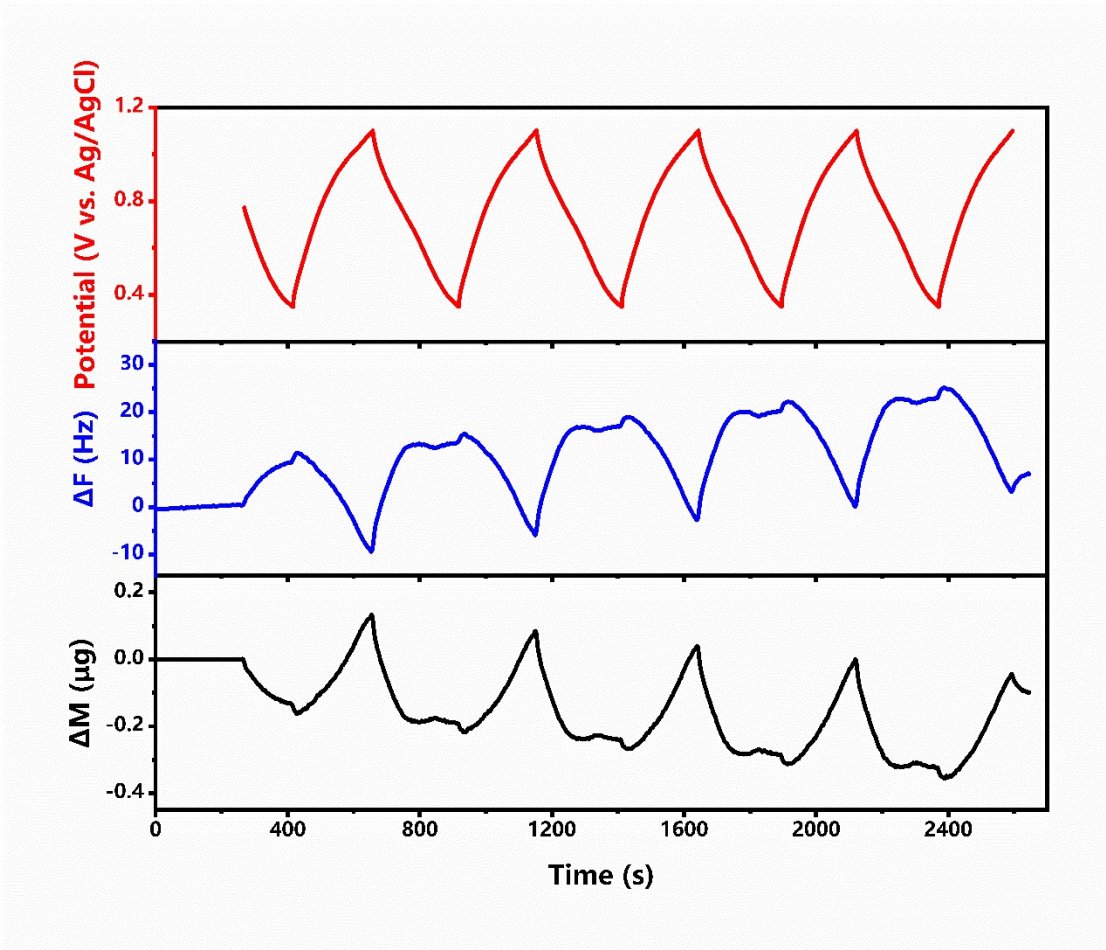

Fig. S11 EQCM analyses of NS-KMnO-coated quartz electrode in 0.5 M K_2SO_4 solution. Here, the changes of potential (red), frequency (blue), and Sauerbrey mass (black) in five cycles are similar, and there is only anion migration during charging and discharging.

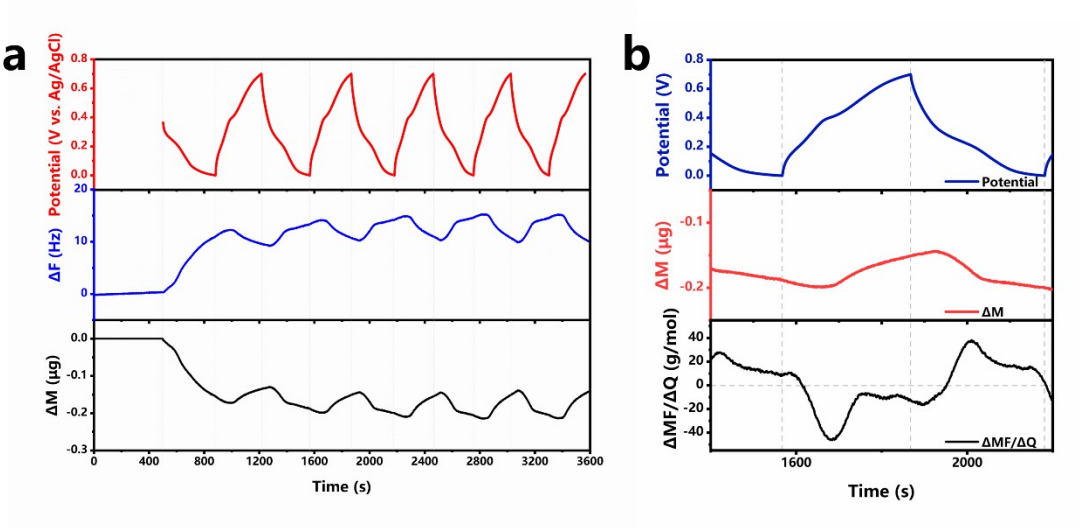

Fig. S12 EQCM analyses of NS-KMnO-coated quartz electrode in 0.5 M CH_3COOK solution. (a) The changes of potential (red), frequency (blue), and Sauerbrey mass (black) in five cycles; (b) The changes of potential (blue), Sauerbrey mass (red), and mass gain or loss rate (black) between the second charge and third discharge. There is anion migration during charging and discharging.

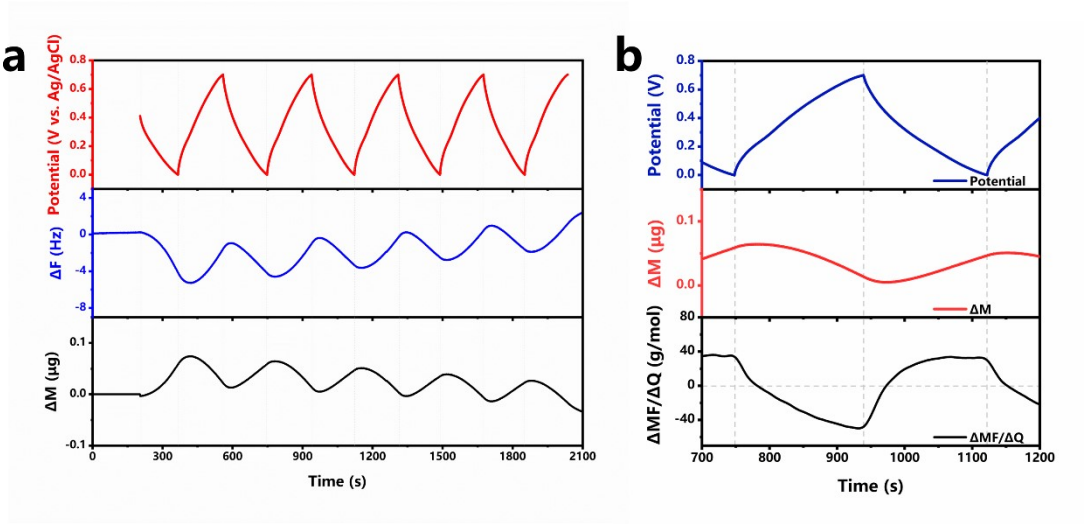

Fig. S13 EQCM analyses of NS-KMnO-coated quartz electrode in 0.5 M KCl solution. (a) The changes of potential (red), frequency (blue), and Sauerbrey mass (black) in five cycles; (b) The changes of potential (blue), Sauerbrey mass (red), and mass gain or loss rate (black) between the second charge and third discharge. There is cation migration during charging and discharging.

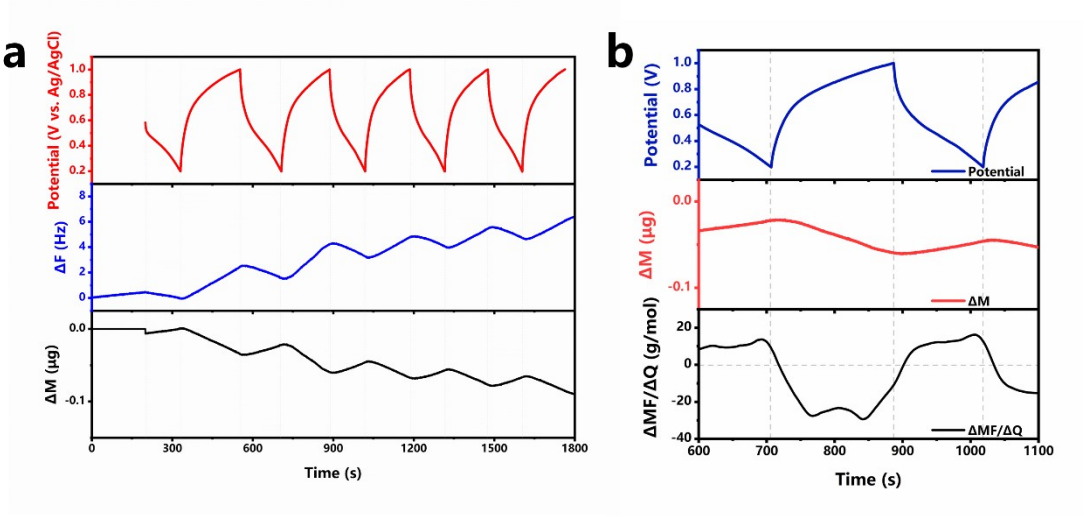

Fig. S14 EQCM analyses of NS-KMnO-coated quartz electrode in 0.5 M KF solution. (a) The changes of potential (red), frequency (blue), and Sauerbrey mass (black) in five cycles; (b) The changes of potential (blue), Sauerbrey mass (red), and mass gain or loss rate (black) between the second charge and third discharge. There is cation migration during charging and discharging.

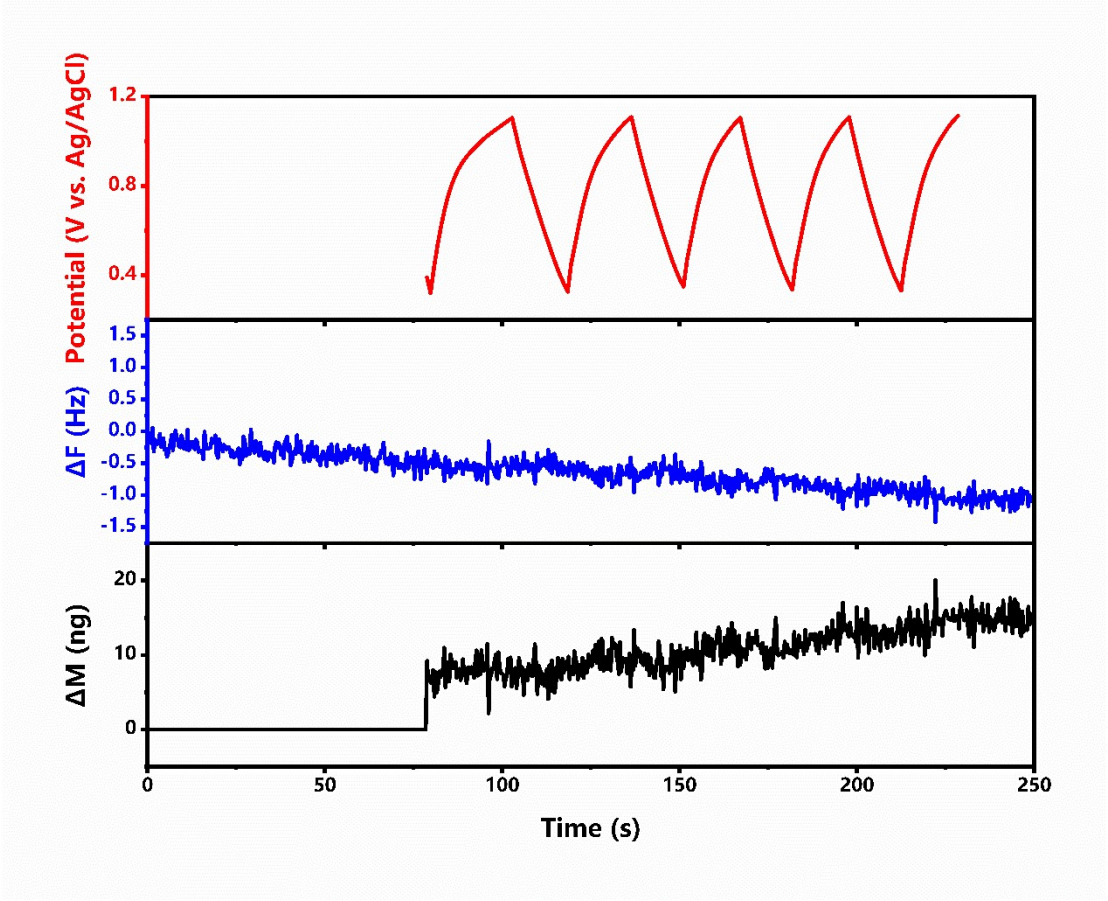

Fig. S15 EQCM analyses of bare quartz electrode in 0.5 M K_2SO_4 solution. The changes of potential (red line), frequency (blue line), and Sauerbrey mass (black line) in five cycles are similar, and there are ng-level Sauerbrey mass fluctuations.

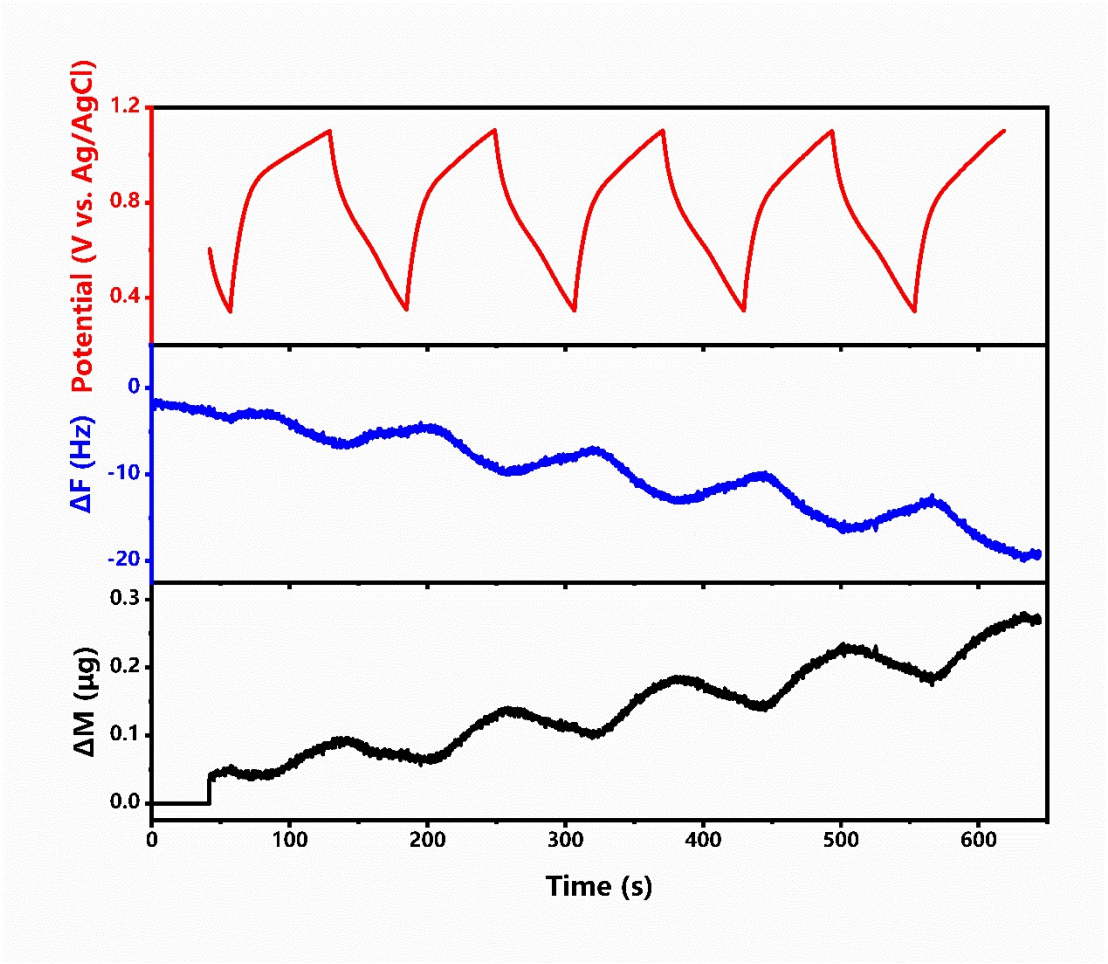

Fig. S16 EQCM analyses of Bulk-KMnO-coated quartz electrode in 0.5 M K_2SO_4 solution. The changes of potential (red line), frequency (blue line), and Sauerbrey mass (black line) in five cycles are similar. A huge Sauerbrey mass change was shown during the CC tests, indicting a low cycle stability.

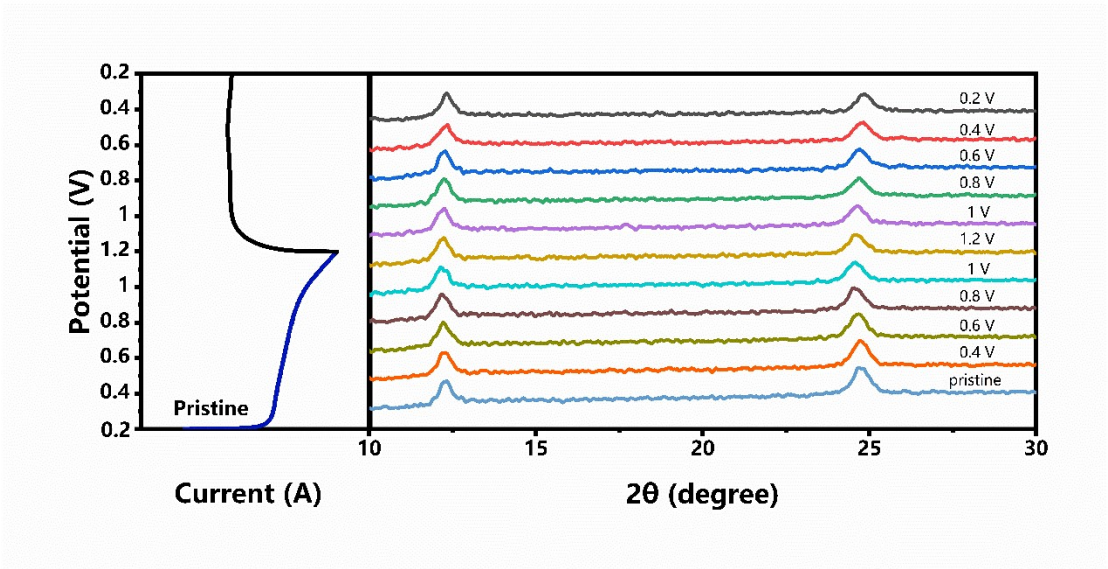

Fig. S17 In-situ XRD date. CV curves of NS-KMnO//YP-50 device at the scan rate of 2 mV s^{-1} (left), corresponding in-situ XRD patterns at different potentials (right).

Table S1 Part of equivalent circuit component fitting value.

materials	R_s (Ω)	C_{dl} (mF)	R_{ct} (Ω)	W_o ($Ω^{-1}$ $s^{0.5}$)	C_l (mF)
NS-KMnO	1.73	3.41	1.95	0.252	431
Bulk-KMnO	2.58	1.06	4.93	0.0294	$1.7x10^{-5}$

References

1. Y. Shao, M. F. El-Kady, J. Sun, Y. Li, Q. Zhang, M. Zhu, H. Wang, B. Dunn and R. B. Kaner, *Chem Rev*, 2018, **118**, 9233-9280.

2. G. Sauerbrey, *Physics*, 1959, **155**, 206-222.